

# Effect of Compressive Residual Stress on the Corner Crack Growth

M.H. Gozin, M. Aghaie-Khafri\*

*Department of Mechanical Engineering, K.N. Toosi University of Technology, Tehran, Iran*

Received 4 May 2013; accepted 17 August 2013

## ABSTRACT

In the present study, plasticity induced crack closure (PICC) concept and three dimensional (3D) finite element methods (FEM) are used to study the effect of compressive residual stress field on the fatigue crack growth from a hole. To investigate the effect of compressive residual stress on crack opening levels and crack shape evolution, Carlson's experiments were simulated. Crack shape evolution is investigated by employing an automatic remeshing technique using MATLAB-ABAQUS code. The effect of mesh element size is considered by using element sizes of 0.025mm and 0.0125mm. Crack opening level results indicate that the applied residual stress increases the opening levels with an average of 45%. The higher opening levels results in higher number of fatigue cycles by a ratio of 3.07 for 1.9mm surface crack growth increment. Comparing the result obtained with Carlson's experiments indicates that the crack closure method employed in the present analysis is in good agreement. Comparing the results with Jones' superposition method, moreover, illustrates that present paper method is more accurate.

© 2013 IAU, Arak Branch. All rights reserved.

**Keywords:** Residual stress; Crack closure; FEM; Crack shape evolution

## 1 INTRODUCTION

THE effect of residual stress on the fatigue crack propagation is of great practical significance and has been the focus of much research. Considering the reliability and operational life of components containing residual stress, it is important to determine the fatigue crack growth under residual stress field. The effect of residual stress on fatigue crack growth has been extensively studied based on the superposition techniques due to their simplicity. In superposition-based techniques, the stresses due to an applied mechanical load are assumed to superimpose linearly on the residual stress. The usage of the superposition has been criticized in view of the fact that it only considers the initial residual stress field that exists in the uncracked structure. The redistribution of the residual stress while the propagating fatigue crack penetrates the residual stress field is neglected. Moreover, it has been pointed out that superposition is invalid while the crack faces contact [1, 2]. Crack closure analysis is a reliable alternative to superposition method in the case of residual stress fields. Elber [3] observed that a crack could be closed even when a tensile load is applied to a specimen. This observation implies that some internal forces hold the crack faces together until the applied tensile load is large enough to separate them. Plasticity-induced crack closure has been recognized as one primary closure mechanism in many engineering situations. It is one of the principal causes of load history effects in crack propagation. It can be used to incorporate crack shielding mechanisms into fatigue crack growth rate models. During fatigue process, PICC occurs due to that the yielded material left in the wake of a crack tip as it propagates through plastic zones. The plastic wake enables the crack to close before

\* Corresponding author. Tel.: +98 09123088389; Fax: +98 21 886 74748.  
E-mail address: maghaei@kntu.ac.ir (M. Aghaie-Khafri).

minimum load is reached. Thus, the effective stress intensity factor range,  $\Delta K_{eff}$ , becomes smaller than the nominal applied range [4, 5] and hence crack propagation is slower than that would be predicted without knowledge of closure. Finite element modeling based on PICC concept has been concerned by many researchers [6-8].

The crack shape development is one of the most important issues when surface cracks subjected to fatigue loads are modeled. In a 3D geometry, the crack opening value will vary along the crack front. This variation will result in that the crack front grows with different rates under the cyclic loading. Consequently, the crack front shape will naturally evolve. This crack shape evolution makes modeling of 3D geometries much more complex [9]. Newman and Raju [10] were the pioneers regarding this problem. They assumed that an initial semi-elliptical surface crack maintains a semi-elliptical shape during the whole propagation. Then, they estimated the growth increments using the Paris law at the free surface and the deepest penetration point of the crack. Connolly and Collins [11] used the alternative current field measurement technique to analyze the shape change of elliptical surface cracks. Mc Fadyen et al. [12] measured the shape evolution of surface cracks with various aspect ratios. They used Newman and Raju's approach to predict the crack aspect ratio variation. Shin [13] studied the crack growth rate and shape development of corner cracks and calibrated the stress intensity factor.

The crack shape development and the crack closure are two factors that interacting each other when a 3D crack propagates. Considering a surface crack, the crack closure effect is more pronounced at the free surface due to the plane stress state. As a result, the crack growth rate at the free surface is reduced and a front-turning-in-ward phenomenon is usually observed. The shape of a crack is primarily considered in the stage of the finite element model development. When the model is established, the initial and the subsequent crack shapes cannot be altered. This is due to that the crack front nodes are simultaneously released. Thus, the evolving crack shape must follow the prescribed mesh arcs. Considering crack closure analysis, the crack front is free and moves without any restraining that arises from prescribed mesh arcs. Hou [14, 15] developed a finite element technique without simultaneously releasing the crack front nodes. This strategy combines the multiple point schemes and the conventional crack closure analysis.

While residual stress can affect the crack shape evolution, numerical elastic-plastic studies in this field is still rare due to complexity of models and time consuming analysis. In the present study, a corner crack growth and the effect of residual stress are investigated using 3D finite element analysis. The interaction of crack closure and crack shape evolution is considered by employing a MATLAB-ABAQUS automatic remeshing code. The effect of residual stress on crack opening levels and crack shape evolution are discussed. Furthermore, the results obtained are compared to Carlson's [16] experiments.

## 2 THE AUTOMATIC REMESHING TECHNIQUE FOR CRACK CLOSURE ANALYSIS

Stress intensity factor at each crack tip node is directly calculated using ABAQUS software. In the present investigation, a finite element technique is developed so that both the crack closure and the crack shape are simultaneously simulated using a MATLAB-ABAQUS interference code. Two finite element models are constructed, one is used to calculate the stress intensity factor at each crack front node and the other is used for the crack closure analysis. Since the first model is utilized for the stress intensity factor calculation, special elements of quartered point are deployed along the front so that the stress singularity can be captured. Hence, the model is analyzed elastically. Elastic-plastic analysis is performed through the second model in a way similar to the conventional closure analysis and the opening stresses ( $S_{op}$ ) at the front nodes are determined.

A MATLAB code was generated to control all crack growth analysis. The code works by constructing ABAQUS input files of the two models and addressing ABAQUS for submitting the analysis. The MATLAB program remains standby while FEM analyses are running. After completion of SIF and closure analysis, the code continues for post processing analysis. Post processing includes obtaining SIF and  $S_{op}$  at each crack front node which leads to calculation of the effective stress intensity factor as following:

$$\Delta K_{eff} = K_{max} - K_{op} \quad (1)$$

where  $\Delta K_{eff}$  is the effective stress intensity range,  $K_{max}$  and  $K_{op}$  are stress intensity factors corresponding to the maximum remote stress and the opening stress, respectively. To determine a new crack shape, the crack front node with the maximum effective stress intensity factor is determined and the crack increment at this node is set to the

maximum predefined crack growth increment at each step. The ratios of other front nodal increments to the increment of the maximum effective stress intensity node are then calculated using the modified Paris law:

$$\frac{da_i}{da_{\max}} = \left( \frac{(K_{\text{eff}})_i}{(K_{\text{eff}})_{\max}} \right)^n \quad (2)$$

where  $da_i$  and  $da_{\max}$  are the crack increments at the front node  $i$  and at the node with the maximum increment, respectively.  $\Delta K_{\text{eff}}$  is the effective stress intensity range and  $n$  is the power exponent of the Paris law. It is worth mentioning that material crack growth data can be directly used instead of Eq. (2).

To calculate fatigue life of the specimen, above crack increments are replaced in Paris law equation:

$$\frac{da_i}{dN} = C(\Delta K_{\text{eff}})_i^n \quad (3)$$

Solving Eq. (3) for  $dN$  and integrating over crack growth increments we have:

$$N = \sum_{i=1}^f dN = \sum_{i=1}^f \frac{da}{C(\Delta K_{\text{eff}})^n} \quad (4)$$

where  $f$  is number of crack growth increments. After calculating  $da_i$  at each crack front node, each node is advanced in the crack plane normal to the crack front. Then, new crack front is defined by a spline which connects new crack tip nodes as is shown in Fig.1. MATLAB sub-code function new crack front.  $m$  is prepared for generation of new crack front. The last part of each crack growth increment is remeshing of the model with the new crack front and transferring history dependent variables from the old mesh to the new one.

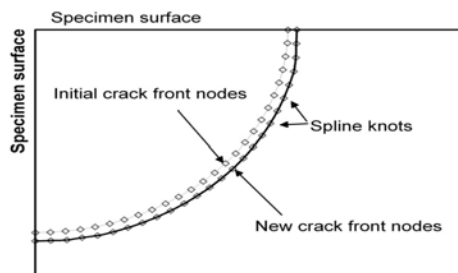


**Fig. 1**  
Crack front advancement and smoothing.

## 2.1 Transferring history dependent variables

Remeshing technique in elastic-plastic models is more complicated than in elastic models [17, 18]. In elastic models state of the stress and strain depends on instantaneous applied loads, boundary conditions and geometry. On the other hand, elastic-plastic analysis is history dependent, and history dependent parameters should be transferred from old mesh to new one [19, 20]. The transfer operation for evolving finite element meshes are provided for the case of a typical elasto-plastic material whose behavior is described by a set of state and internal variables. Once a new mesh is generated, state and internal variables need to be mapped from the old finite element mesh to the new one. The state variables consist of the nodal displacements  $u$  and the integration point variables include the Cauchy stress tensor  $\sigma$ , the strain tensor  $\varepsilon$ , the plastic strain tensor  $\varepsilon_p$  and a vector of internal variables  $q$  [21]. It must be noted that the transfer of the complete state array would result in the data that may not be self-consistent. For instance, the yield condition  $f(\sigma, q)=0$  may not be satisfied. In fact, the set of internal variables  $\varepsilon_p, q$  prescribed at each Gauss point characterizes in full the history of the material on the new mesh. These internal variables provide sufficient information for computation of a new solution [21].

Several works concerning fields mapping in the scope of nonlinear mechanics and remeshing processes can be found in the literature [22]. The most usual method consists of extrapolation the field to the nodes of the old mesh then, interpolating those values to the integration points of the new mesh using shape functions (standard interpolation technique). ABAQUS employs the standard interpolation technique with the module named mesh-to-mesh solution mapping. An initial step should be defined to allow Abaqus to check for equilibrium. Then, the interpolation can be done. By default, Abaqus resolves the stress unbalance linearly over the step. Automatic remeshing MATLAB code developed by the authors is supported with standard interpolation algorithm using ABAQUS mesh-to-mesh solution mapping module.

Transferring history dependent variables is the last part of each crack growth increment. At the end of this step, MATLAB code loop is completed and new FEM analysis for calculation of SIF and  $S_{op}$  at the new crack front nodes is simulated. The loop continues till the crack reaches its predefined final length. This technique is schematically depicted in Fig.2.

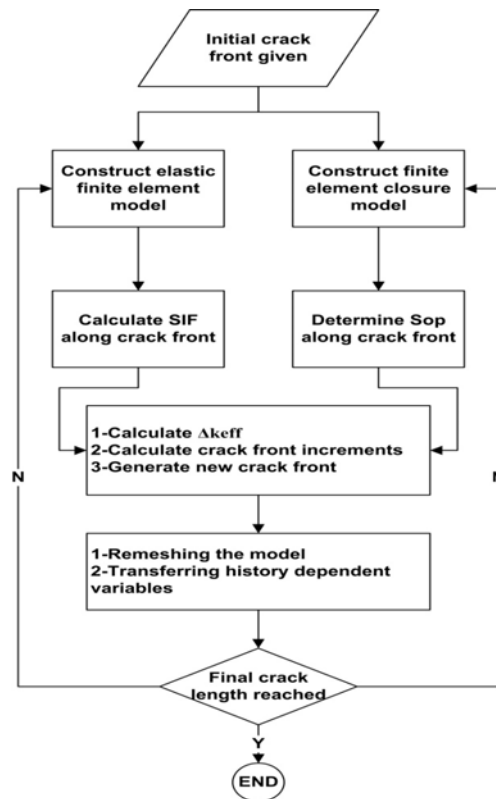


Fig. 2  
Crack shape evolution methodology perspective.

### 3 MATERIAL SPECIMEN AND TESTS

Fatigue crack growth from a cold worked hole in a sheet has been studied by many researchers [23]. Liu [24] measured fatigue part through crack growth rates from pre-yielded holes in aluminum AA2024-T351 sheets. LaRue and Daniewicz [23] analyzed Liu's experiments with a  $\Delta K_{eff}$  approach, but used 2D elasto-plastic finite element analysis of the actual cracked specimen under repeated loading and unloading to solve for  $K_{open}$ . The  $\Delta K_{eff}$  life predictions again correlated well with Liu [24] data, within a factor of 1.2. Gozin and Aghaie-Khafri [25] applied  $\Delta K_{eff}$  approach to Liu's model using both 2D and 3D finite element analysis. Their simulation results were fairly well correlated with experimental data. Gozin and Aghaie-Khafri modified the PICC method by introducing a correction factor to crack opening load value. The method reduced the 3D FEM fatigue life prediction errors.

Jones [26] predicted the fatigue propagation of corner cracks from cold worked holes using 3D finite element models with superposition method. Jones' [13] models account for the through thickness variation in residual stress left after cold working. Predicted fatigue lives and crack front shapes are compared to the experimental results of

Carlson [16] in aluminum 2024-T351, and Pilarczyk in aluminum 7075-T651 [16]. Jones [26] shows the evolution of P-shaped crack fronts similar to those observed in the experiments. Predictions based on the initial residual stress field left after cold working are non conservative, predicting either slower than experimental crack growth or crack growth that arrests. In the present work, the crack growth model is the same as Carlson [16] fatigue tests on AA2024-T351. The chemical composition of AA2024 consisted of 0.5% Fe, 0.6% Mn, 0.5% Si, 4.1% Cu, 1.3% Mg, 0.25% Zn and the balance being aluminum. As a base line for fatigue crack growth behavior, Carlson's test specimens were almost manufactured out of the same basic material blank as the ASTM E647 specimens. However, in the Carlson's test specimen one 2.54 mm hole and two through-thickness EDM notches in the center of the test specimen were replaced by a center hole and an EDM corner notch, as is shown in Fig. 3. Tensile properties and crack growth data of AA2024-T351 are shown in Fig. 4 and Fig.5. Regarding to Fig.4, bilinear stress-strain curve is applied for elastic-plastic finite element analysis.

In the present study, two models are considered. The first model performed crack growth analysis without the simulation of cold working effect. The second model consists of the simulation of cold working effect based on the Carlson's experiments. Therefore, the effect of residual stress on crack opening levels and crack shape evolution is investigated.

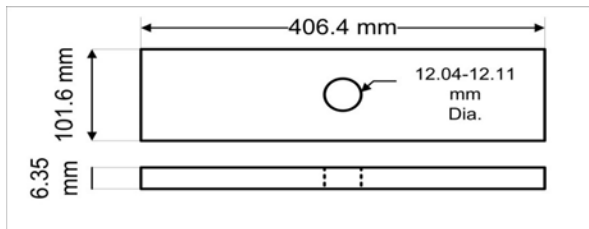


**Fig. 3**  
Carlson's [16] experiments specimen.

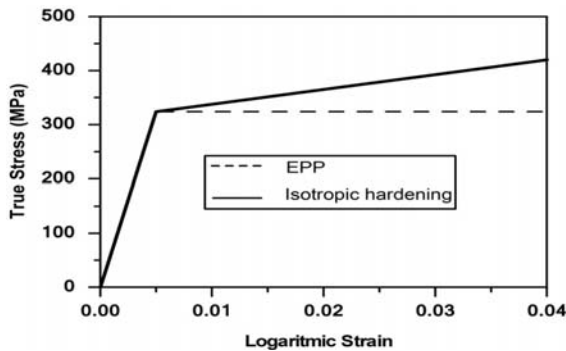


**Fig. 4**  
Stress-strain behavior of AA2024-T351, where EPP stand for elastic perfect plastic.

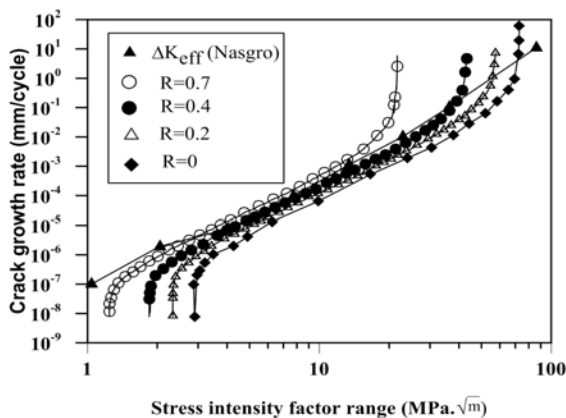


**Fig. 5**  
Crack growth data for AA2024-T351.

## 4 FINITE ELEMENT ANALYSIS

### 4.1 cold work simulation

Finite element simulation of the cold working process is the same as Carlson's [16] experiments. The residual stress field is introduced using cold working process. The cold working process is applied according to the Fatigue Technology Inc. (FTI) split sleeve cold working method [28]. The process consists of using a hardened, stainless-steel and internally lubricated split sleeve which is pulled over a tapered mandrel through the hole. This causes very high radial pressures that expand the hole beyond the yield strength, resulting in a residual compressive stress after the mandrel removal.

When the actual method of cold work is used, where a tapered mandrel is drawn through the hole, a variation of the residual stress through the thickness is obtained [29]. The applied interference is given by:

$$i = \frac{(\bar{D} + 2t - SHD)}{SHD} \times 100\% \quad (5)$$

where  $\bar{D}$  is the major mandrel diameter,  $t$  is the sleeve thickness and SHD is the starting hole diameter. Mandrel and sleeve dimensions presented in Fig. 6 and Fig. 7 show a quarter of the 3D finite element model and some details of the assembly components. Frictionless conditions are assumed between the mandrel and sleeve, and between the sleeve and the aluminum alloy plate. The assumption of frictionless contact is justified because the sleeve is lubricated. A linear elastic model is used for the sleeve with an elastic modulus of 210GPa and Poisson's ratio of 0.3. The mandrel is modeled as a rigid part. The part shown in Fig.7a has 22130 linear hexahedral elements.

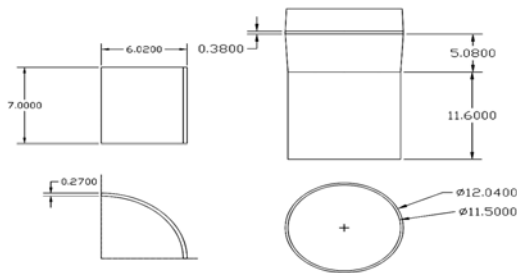


**Fig. 6**  
Sleeve and mandrel dimensions.

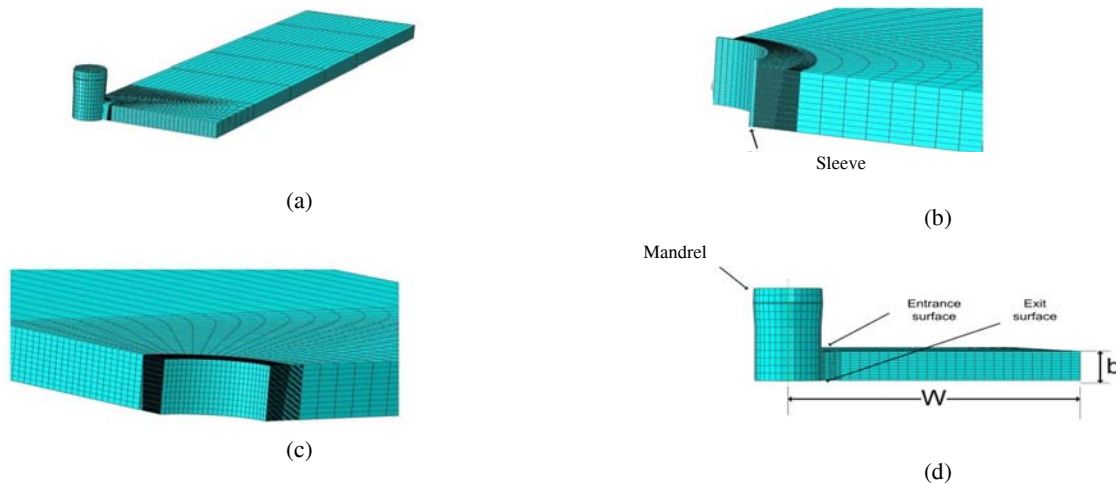


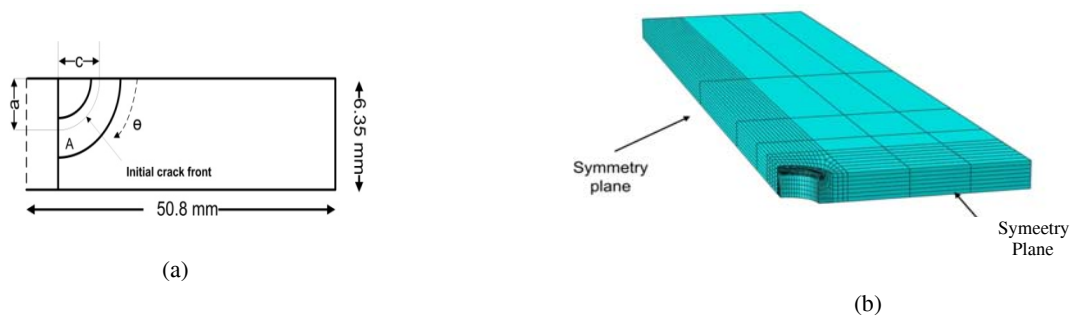
**Fig. 7**  
3D finite element model of a) cold work system assembly, b) split sleeve contact with part and c) part mesh generation around the hole, d) dimension labels.

The contact between the hole surface and the sleeve, and also between the sleeve and the mandrel is modeled. A frictionless contact is assumed between the contacting surfaces. Ten elements along the plate thickness are used. Previous work [29] has shown that considerable refinement of the mesh on the surface of the plate and in the vicinity of the edge of the hole is required. At the end of split sleeve cold working, the specimen is subjected to a reaming process to the final hole diameter of 12.7 mm. The reaming process is modeled using element delete option in ABAQUS 6.11. Table 1 indicates the parts specification for cold work modeling.

#### 4.2 crack closure simulation

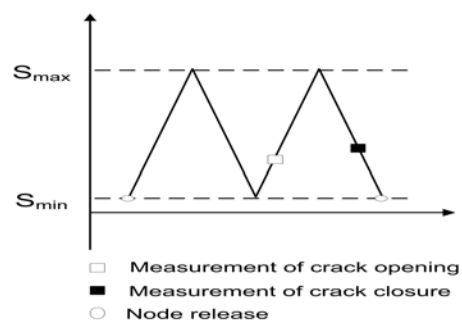
For both cold worked and non-cold worked models, the finite element model for crack closure analysis consists of 20-noded hexahedral elements (quadratic elements) with reduced integration. To simulate the stress-strain behavior of the material, bilinear elastic-plastic model is considered and the von-mises yield criterion is implemented. Based on Carlson's [16] experiments, two types of cracks initiate in the specimens. Primary crack initiates from EDM notch with an initial size of  $0.789 \times 0.764$  mm at the entrance surface edge of the part hole, Fig.8. Secondary cracks automatically initiate at the opposite edge of the hole after some amount of crack growth with approximately same length. Concerning specimen symmetry,  $\frac{1}{4}$  of the sample is modeled. Mesh refinement procedure is used around the crack tip region to approach convergence of 1.15 MPa for element length of 0.0125 mm. The finite element model of initial crack size of  $0.789 \times 0.764$  consists of 9806 elements and 43809 nodes. Clearly, mesh parameters change as the crack grows. The loading condition consists of remote tensile stress of 172.25 MPa with stress ratio of  $R=0.1$ .

Crack closure is predicted by monitoring the contact between crack faces. A rigid plate in the plane of crack tip is considered and a frictionless contact between crack faces and rigid plate is defined to prevent crack faces penetration. The model is incrementally loaded to the maximum load and then unloaded to the minimum load, where the crack tip node is released (due to convergence issues) and allowing the crack to advance. The nodal displacement of the first node that is located behind the crack tip is monitored. Between any two increments, if the nodal displacement became positive, the crack is assumed open. Fig.9 shows that nodes are released and remeshing is performed.



**Fig. 8**

(a) Dimensions of the crack plane and the mesh plan, and (b) finite element meshes of the analyzed specimen.



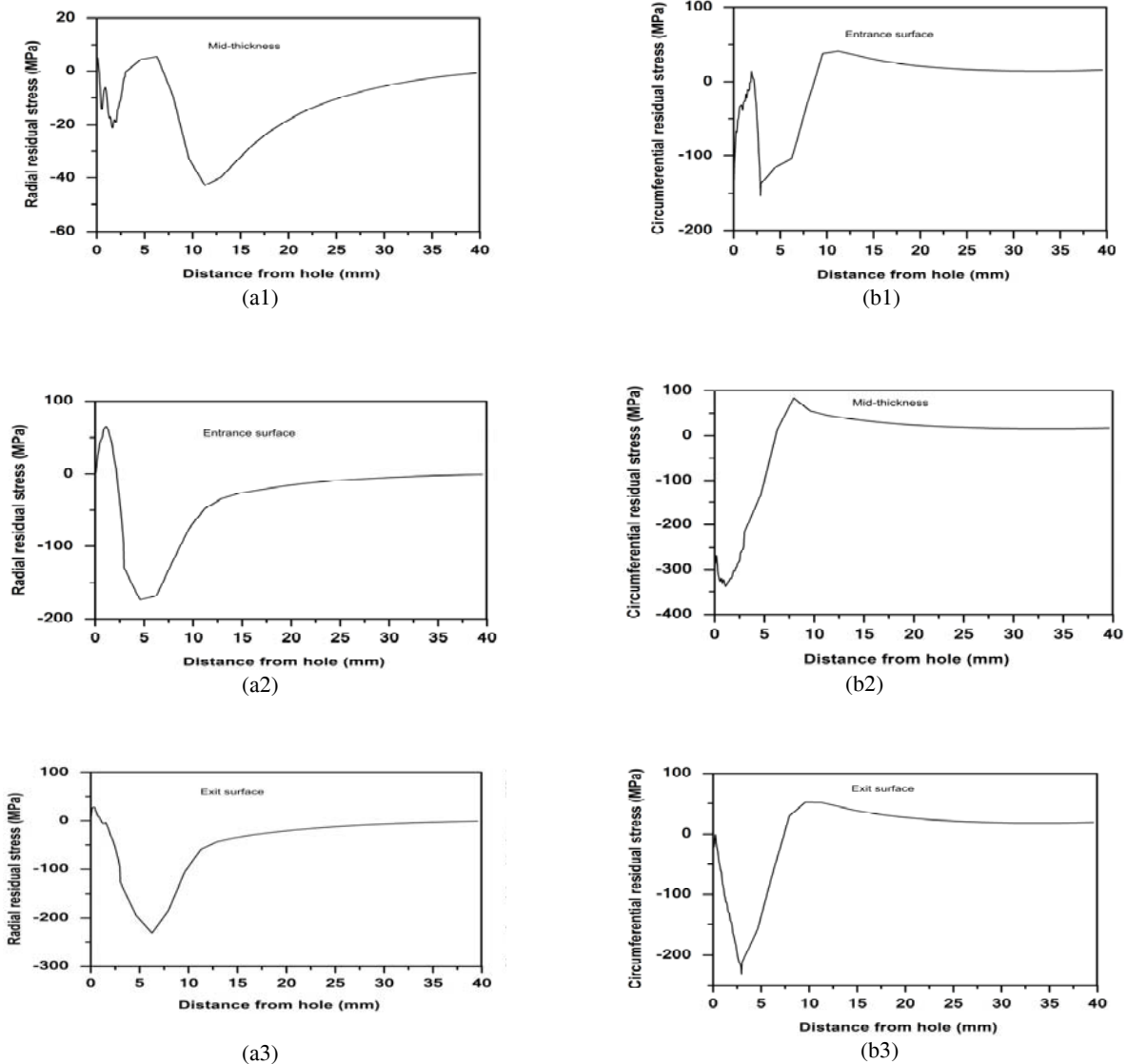
**Fig. 9**

Illustration of the node release scheme for the finite element model and points at which the opening and closure are measured during load cycling.

## 5 RESULTS AND DISCUSSION

### 5.1 Residual stress distribution

The residual stress fields are presented in Fig. 10 for the entrance, mid-thickness and exit faces. Stress variations through part thickness highlight the importance of using 3D FEM for the residual stress analysis. Residual stress distribution indicates that higher compressive residual stress values are developed as the mandrel goes down through exit surface. The maximum compressive circumferential residual stress occurs at the mid thickness with a value of 345 MPa at 1.1mm distance to the bore. However, the maximum tensile circumferential residual stress occurs at the mid thickness with a value of 75 MPa at 7.5mm distance to the bore.



**Fig. 10**

Residual stress distribution after cold work (a) Radial (a1) entrance face; (a2) mid-thickness; (a3) exit face; and (b) circumferential (b1) entrance face; (b2) mid-thickness; (b3) exit face residual stresses fields.



### 5.2 Mesh refinement study

When accuracy of opening loads is significant in crack closure analysis, an important criterion for mesh refinement is the number of elements that yielded at the crack tip. Two different types of crack tip plastic zones are generated due to fatigue crack propagation. The first is forward plastic zone which is the plastically deformed material near the crack tip undergoing the maximum load. The second zone of interest is the reversed plastic zone, which is defined as the material near the crack tip undergoing compressive yielding at the minimum load [6].

Solanki et al. [30] indicated that approximately 3-4 elements are required in the reversed plastic zone to obtain accurate opening load values. Variations of elements number in forward and reversed plastic zones are listed in Table 1. It can be observed that plastic zone sizes at crack edges are larger due to the plane stress condition at the free surface of the part. Considering the results of Table 2. , just for  $d_a=0.0125\text{mm}$  the number of elements in the reversed plastic zone is at least equal to 3 for all portions of the crack.

**Table1**

Cold work specimen details

Material	AA2024-T351
Specimen name	CX-2024-4
W	50.8 mm
b	6.35 mm
Hole size before CX	12.05 mm
Sleeve size before CX	0.27 mm
Mandrel diameter	12.04 mm
Applied expansion	3.6 %
Hole size after expansion	12.35 mm
Hole size after reaming	12.7 mm

**Table2**

Variation of number of elements in plastic zones with mesh refinement

Element size (mm)	Forward plastic zone			Reversed plastic zone		
	Surface	Mid-thickness	Bore	Surface	Mid-thickness	Bore
0.1	3	2	3	1	0	0
0.05	5	4	5	1	0	0
0.025	10	6	8	4	1	2
0.0125	14	8	10	6	3	4

### 5.3 Crack growth simulation results

Crack opening levels for different models are shown in Fig. 11 and Fig.12. The results indicate that for no residual stress model, opening levels at the surface and at the bore are higher than the mid thickness.

The effect of mesh refinement on crack opening is considered using three mesh element sizes of 0.05mm, 0.025 mm and 0.0125mm. Referring to the previous section results, only 0.0125mm element size can be used for crack closure analysis. Considering Fig. 11, decreasing element size from 0.05mm to 0.0125mm results in higher opening levels at all crack regions. The difference between 0.05mm and 0.025mm stabilized opening levels is 20%. However, decreasing element size from 0.025mm to 0.0125mm results in just 5% difference. In the case of no residual stress, stabilized opening levels are 0.54, 0.2 and 0.62 for surface, mid thickness and bore, respectively. Following compressive residual stress, crack opening level pattern changed. Compressive residual stress decreases the effect of plane stress at the surface and at the bore as is shown in Fig.12. Variation of opening levels highly depends to applied residual stress at lower crack lengths. Following 0.5 mm of crack growth, crack opening levels depends on two parameters. The first one is the residual stress distribution and the second one is the plastic wake due to loading and unloading. Comparing opening levels in Figs. 11 and 12, it can be concluded that the normalized opening stress is increased 45% due to the effect of residual stress. The maximum increase in the opening stress occurs at the mid-thickness and at no residual stress situation where plane strain condition results in much lower opening stress.

The result of crack shape simulation based on the elastic-plastic remeshing technique is shown in Fig.13. It can be observed that a same initial crack shape evolves to different shape following only 2.5 mm of crack growth. This is as a result of compressive residual stress field. It is observed that the continuously higher opening level near the surface and the bore (Fig. 7) deviates the front and to turn it inward. Applying residual stress to the model, results in different shape evolutions. Higher opening stress levels at the mid thickness give rises to decrease in plane stress effect particularly at the bore.

5.4 Fatigue life predictions

Fatigue life predictions for a 2.5mm crack growth using automatic remeshing technique are shown in Fig.14. The results indicate that cold work process increases the number of fatigue cycles by a factor of 3.07. Carlson’s [16] experiments conducted 12 crack growth tests with same fatigue and cold working parameters. Thus, in Fig.14 all fatigue life results are plotted at the point of 1.9mm crack length. Considering Fig.14, some scatter in Carlson [16] test is observed. This scatter in fatigue cycles proves that the fatigue life depends on many other parameters such as loading conditions and cold work process. Average fatigue cycles of Carlson’s [16] tests at 1.9 mm crack length is 54671, which is 20% higher than the results of the present analysis. The result indicates that crack closure method used in this investigation is conservative. This is also observed in the previous crack closure studies [23, 25].

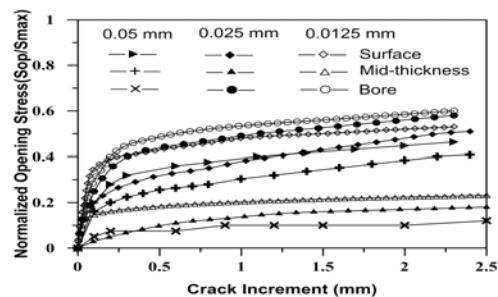


Fig. 11 Normalized crack opening stress obtained from crack closure finite element model without residual stress.

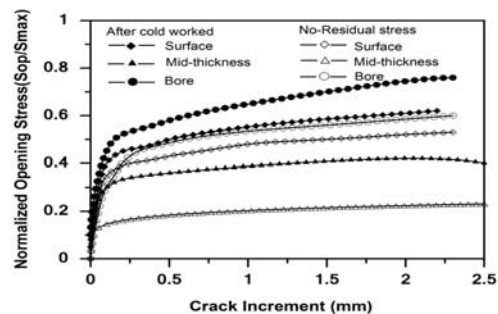


Fig. 12 Comparison of crack opening stress levels obtained from two crack closure finite element models with and without residual stress.

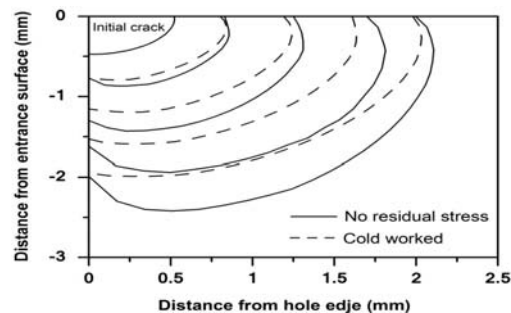
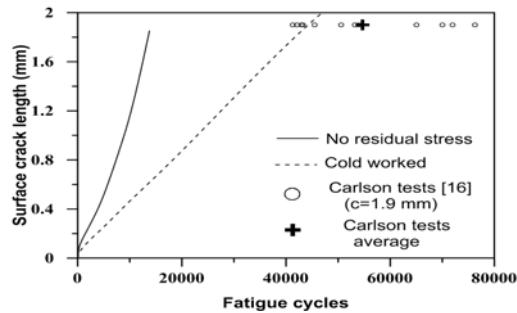


Fig. 13 Comparison of crack shape evolution levels obtained from two crack closure finite element models with and without residual stress.

**Fig. 14**

Effect of cold working on predicted fatigue cycles and comparison with Carlson's results [16].

## 6 CONCLUSIONS

In the present paper, effects of compressive residual stress on crack opening stress levels, crack shape evolution and number of fatigue cycles are investigated using 3D finite element modeling of a corner crack emanating from a hole. A finite element technique is developed so that both the crack closure and the crack shape are simultaneously simulated using a MATLAB-ABAQUS interference code. The following issues can be concluded from the analysis.

- Distribution of residual stress due to cold expansion of hole highlights the importance of 3D finite element modeling for residual stress analysis.
- Increasing number of elements around the crack tip region would give rise to increase in captured crack opening stress levels at all portion of the crack tip.
- Higher opening stress levels are observed at the surface and at the bore region due to plane stress conditions.
- Applying compressive residual stress to the model using cold work simulation, results in approximately 45% increase in normalized opening stress values.
- Plane stress condition at the free surface give rises to front-turning-inward for no residual stress condition. Compressive residual stress decreases this effect.
- Comparing fatigue life predictions to average number of cycles of Carlson's tests indicates that predictions are acceptable by 20% error while Carlson's test results scatters by more than 50%.

## REFERENCES

- [1] Jones K.W., Dunn M.L., 2009, Predicting fatigue crack growth from a preyielded hole, *International Journal of Fatigue* **31**:223-230.
- [2] Parker A.P., 1982, Residual stress effects in fatigue, *ASTM STP 776, American Society for Testing and Materials* 13-31.
- [3] Elber W., 1970, Fatigue crack closure under cyclic tension, *Engineering Fracture Mechanics* **2**:37-45.
- [4] Elber W., 1971, The significance of fatigue crack closure damage tolerance in aircraft structures, *ASTM STP486, American Society for Testing and Materials* 230-242.
- [5] Schijve J., 1988, Fatigue crack closure: observations and technical significance mechanics of fatigue crack closure, *ASTM STP 982, American Society for Testing and Materials* 6-34.
- [6] Solanki K., Daniewicz S.R., Newman J.C., 2004, Finite element analysis of plasticity-induced fatigue crack closure: an overview, *Engineering Fracture Mechanics* **71**:149-171.
- [7] McClung R.C., Sehitoglu H., 1989, On the finite element analysis of fatigue crack closure-1. basic modeling issues, *Engineering Fracture Mechanics* **33**:237-252.
- [8] Ismonov S., Daniewicz S.R., 2010, Simulation and comparison of several crack closure assessment methodologies using three-dimensional finite element analysis, *International Journal of Fatigue* **32**:1322-1329.
- [9] Chermahini R.G., Blom A.F., 1991, Variation of crack-opening stresses in three-dimensions: finite thickness plate, *Theoretical and Applied Fracture Mechanics* **15**:267-276.
- [10] Newman J.C., Raju I.S., 1981, An empirical stress-intensity factor equation for the surface crack, *Engineering Fracture Mechanics* **15**:185-192.
- [11] Connolly M.P., Collins R., 1987, The measurement and analysis of semi-elliptical surface fatigue crack growth, *Engineering Fracture Mechanics* **26**:897-911.
- [12] Mc Fadyen N.B., Bell N.B., Vosikovskiy O., 1990, Fatigue crack growth of semi-elliptical surface cracks, *International Journal of Fatigue* **12**:43-50.

- [13] Shin C.S, 1991, Some aspect of corner fatigue crack growth from holes, *Journal of Fatigue* **13**:233-240.
- [14] Hou C.Y., 2008, Simultaneous simulation of closure behavior and shape development of fatigue surface cracks, *International Journal of Fatigue* **30**:1036-1046.
- [15] Hou C.Y., 2011, Simulation of surface crack shape evolution using the finite element technique and considering the crack closure effects, *International Journal of Fatigue* **33**:719-726.
- [16] Carlson S.S., 2008, *Application of Beta Corrections to Model and Predict fatigue Crack Growth at Cold Expanded Holes in 2024-T351 Aluminum alloys*, M.S. Thesis, The University of Utah.
- [17] Anderson T.L., 2004, *Fracture Mechanics: Fundamentals and Applications*, CRC press.
- [18] Broek D., 1982, *Elementary Engineering Fracture Mechanics*, Martinus Nijhoff Publishers.
- [19] Hasanov A., Seyidmamedov Z.M., 2007, A finite element analysis and remeshing algorithm for an axisymmetric elastoplastic contact problem related to indentation measurements, *Materials & Design* **28**:62-70.
- [20] Maligno A.R., Rajaratnam S., Leen S.B., Williams E.J., 2010, A three-dimensional (3D) numerical study of fatigue crack growth using remeshing techniques, *Engineering Fracture Mechanics* **77**:94-111.
- [21] Khoei A. R., 2005, *Computational Plasticity in Powder Forming Processes*, Elsevier Ltd.
- [22] Hamel V., Roelandt J.M., Gacel J. N., Schmit F., 2000, Finite element modeling of clinch forming with automatic remeshing, *Computers and Structures* **77**:185-200.
- [23] LaRue J.E., Daniewicz S.R., 2007, Predicting the effect of residual stress on fatigue crack growth, *International Journal of Fatigue* **29**:508-515.
- [24] Liu A.F., 1979, The effect of residual stresses on crack growth from a Hole., *Northrop Corporation Aircraft Group* 74-79.
- [25] Gozin M.H., Aghaie-Khafri M., 2012, 2D and 3D finite element analysis of crack growth under compressive residual stress field, *International Journal of Solids and Structures* **49**:3316-3322.
- [26] Jones K.W., 2009, *Predicting Fatigue Crack Growth Through Residual Stress Fields*, Ph.D. Thesis, University of Colorado.
- [27] Pilarczyk R., 2008, *Beta Corrections to Predict Fatigue Crack Growth at Cold Expanded Holes in 7075-T651 Aluminum Alloy*, M.Sc. Thesis, The University of Utah.
- [28] Fatigue Technologies Inc, 2002, *Cold Expansion Holes Using the Standard Split Sleeve System and Countersink Cold Expansion*.
- [29] Pavier M.J., Ponssard C.G.C., Smith D.J., 1998, Finite element modelling of the interaction of residual stress with mechanical load for a crack emanating from a cold worked fastener hole, *The Journal of Strain Analysis for Engineering Design* **33** (4):275-289.
- [30] Solanki K., Daniewicz S.R., Newman J.C. 2004, A new methodology for computing crack opening values from finite element analyses, *Engineering Fracture Mechanics* **71**:1165-1175.